
Supplementary Material for

ProBio: A Protocol-guided Multimodal Dataset for Molecular Biology Lab

Jieming Cui^{*,1,2}, Ziren Gong^{*,5}, Baoxiong Jia^{*,2},
Siyuan Huang², Zilong Zheng², Jianzhu Ma^{3,4}, Yixin Zhu¹

¹ Institute for Artificial Intelligence, Peking University

² National Key Laboratory of General Artificial Intelligence, BIGAI

³ Department of Electronic Engineering, Tsinghua University

⁴ Institute for AI Industry Research, Tsinghua University

⁵ School of Transportation Science and Engineering, Beihang University

<https://probio-dataset.github.io>

1 Our project page is <https://probio-dataset.github.io>

2 A Data

3 In this section, we will introduce our dataset construction process in two parts: data collection and
4 data annotation. This includes clarifications on data sources, collection methods, annotation tools, *etc.*
5 We present in detail as follows:

6 A.1 Data Collection

7 **Did you include the estimated hourly wage paid to participants and the total amount spent**
8 **on participant compensation?** Yes, we did. Prior to the annotation and human study process,
9 compensation was prearranged and discussed with the participating individuals. A labor fee of 100
10 RMB per 30 minutes will be remunerated to them, with any duration less than 30 minutes being
11 considered as half an hour. The aggregate labor charges for all individuals involved sum up to 5,000
12 RMB.

13 A.1.1 Biology protocol

14 In order to ensure the precision and comprehensiveness of biological protocol data, the initial
15 step involves the retrieval of a substantial number of protocols from highly regarded journals and
16 conferences such as Cells (MDPI, 2011), Jove (JOVE, 2006), and Protocol Exchange (NATURE,
17 2000) for the period spanning 2022 and prior years. The aforementioned protocols represent the
18 forefront of experimental guidelines within the realm of biology and serve as a highly appropriate
19 foundation for establishing a standardized protocol for biological experimentation. The microscopic
20 realm is the setting for certain biological experiments, including brain neuroscience and genetic
21 sequencing, which are not discernible to the unaided eye. In light of this, we have identified 12,381
22 experiments that are amenable to oversight via a monitoring system.

23 The experimental protocols procured from high-ranking academic journals are notably succinct, with
24 most protocols offering mere guidance without practical operational steps (Ioannidis, 2005; Begley
25 and Ellis, 2012). Hence, they are denoted as brief experiments, commonly abbreviated as `brf_exp`.
26 To render these succinct and theoretical procedures feasible, it is imperative to deconstruct them and

*indicates equal contribution.

33 accuracy and completeness. As a result, the protocols that were previously only instructive in nature
34 can now be executed.

35 An online annotation tool has been developed to streamline the annotation process for annotators
36 across the globe and facilitate real-time multiple rounds of mutual checks. We track the information
37 of annotators and modifiers through IDs, aiming to improve the efficiency and standardization of the
38 annotation process. The instructions for using the annotation interface and tools are shown in Fig. 1.

39 A.1.2 Monitoring video

40 To gather a comprehensive video collection, we have established a partnership with an internationally
41 recognized biological laboratory that adheres to standard protocols [Nest.Bio Labs \(2023\)](#). This
42 collaboration enables us to capture the various activities involved in conducting biology experiments.
43 This category of laboratory adheres to an international standard that mandates uniformity in both the
44 interior and exterior appearance and design across laboratories worldwide. Unified regulations dictate
45 the number, color, and size of workstations, the height of the ceiling, and the dimensions of the rooms.
46 This offers a superb opportunity to broaden the global impact and augment the applicability of our
47  ProBio.

48 Under the supervision of experienced researchers, we conducted the process of laboratory selection
49 and camera setup. The selected molecular biology laboratory comprises seven primary experimental
50 stations, a refrigeration unit, and a sterile enclosure. To ensure comprehensive coverage of all
51 operations and instruments, we deployed ten high-resolution cameras strategically positioned from a
52 top-down perspective to minimize occlusion. Every experimental table, refrigerator, and chamber is
53 furnished with a specialized camera for the purpose of documentation. An additional camera has been
54 installed with a specific focus on the frequently utilized water bath during experimental procedures,
55 in order to guarantee that no procedural details are impeded or overlooked during the water bath
56 process. Furthermore, we positioned a single RGB-D camera in proximity to the experimental
57 table and sterile chamber to record operations with a higher level of detail and a closer perspective.
58 Following the completion of the setup, a continuous and uninterrupted silent recording plan was
59 implemented for the ongoing experimental operations, with the aim of minimizing any potential
60 impact on the experimenters. The raw video footage collected for this study exceeded a total of
61 700 hours. Subsequently, the dataset was generated via post-processing techniques and annotation
62 procedures.

63 A.2 Data Annotation

64 Before annotation, we use the semi-automated method to remove irrelevant video clips, such as clips
65 with no human, clips with unrelated actions, *etc.* In the semi-automated filtering process, we apply
66 YOLOv5 ([Ultralytics, 2022](#)) and OpenPose ([Cao et al., 2017](#)) to crop key video clips with related
67 experiment instructions and operations. We then manually remove frames depicting actions unrelated
68 to the intended focus, such as conversing, note-taking, or texting. In order to ensure the efficiency
69 of pre-processing, we carefully check each clip of our filtered videos. Finally, we obtain a total of
70 180.6h videos.

71 A.2.1 Alignment

72 In the process of data collection, a total of 12,381 brief experiments were acquired along with their
73 respective practical experiments following necessary adjustments and completion. Additionally, we
74 obtained a collection of raw videos spanning 180.6h, however, no connection was established between
75 this particular dataset and the aforementioned data type. To establish the correlation between the
76 aforementioned modalities, a team of master’s and doctoral students from prestigious academic
77 institutions such as Peking University, Tsinghua University, and Peking Union Medical College
78 Hospital were recruited to conduct alignment annotation. The task of annotation entails establishing a
79 correspondence between the present state of videos and practical experiments (*i.e.* `prc_exp`) through
80 the allocation of action labels, thereby enabling the subsequent annotation of more detailed actions.

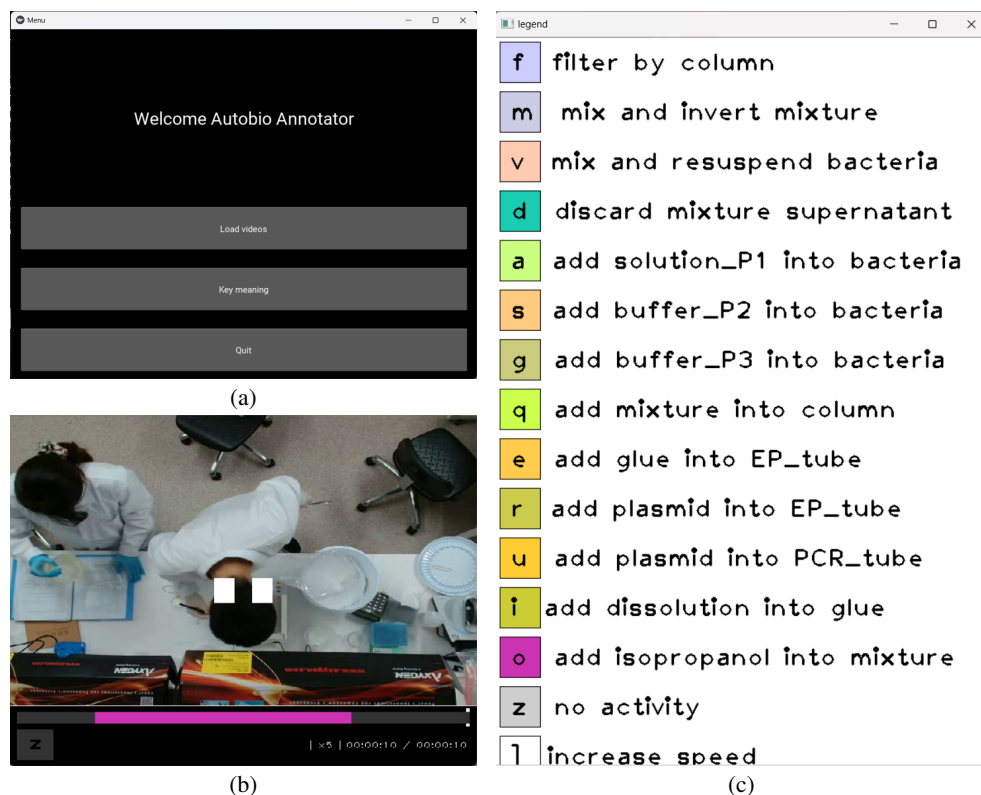


Figure 2: (a) The main page of our tool. (b) Main interface for playing videos at variable speeds. (c) List of `prc_exp` of the chosen `brf_exp`.

81 An offline video action annotation tool has been developed to enhance the annotation process for
 82 annotators located in various regions. The tool, depicted in Fig. 2, enables the application of diverse
 83 labels through the use of keyboard shortcuts, thereby enhancing the efficiency of the annotation
 84 process. In the course of annotating alignments, we have ascertained that the periodic occurrence of
 85 routine operations is a common phenomenon. Consequently, we opted to engage in a collaboration
 86 with expert experimenters to carefully choose a subset of video frames from the existing footage for
 87 further detailed annotations.

88 A.2.2 Fine-grained annotation

89 Then, we employ a team of annotators and provide a two-day professional training on all Molecular
 90 Biology Lab (BioLab) instruments, solutions, and operations. After the training, we divide the current
 91 video into multiple batches of 30-50 minutes each and deliver them iteratively to the annotation
 92 team. Before each batch delivery, we provide corresponding annotation guidelines, including the IDs
 93 of the experimental personnel, the items involved in the operation, and their respective labels. We
 94 create the dataset through real-time acceptance of online annotations. After completing 12 batches
 95 of annotations, we have annotated 213,361 segmentation maps for 10.69h and summarized two
 96 characteristics in our dataset: (i) Many operations involve the combination of multiple transparent
 97 solutions to yield a new transparent solution. In experimental settings, it is customary to employ
 98 transparent and uncolored apparatus and solutions. (ii) Similar movements represent entirely different
 99 jobs and lead to divergent purposes, which is named ambiguity.

100 **Solution status** In view of the two main characteristics of this dataset, while also considering the
 101 huge number of segmentation maps, we divide the dataset into two major parts. We first annotate
 102 1.05h videos for learning more about transparent objects and solutions. Following consultation with
 103 experienced experimenters, we collect 48 object categories and 12 solution categories. Instance masks
 104 and bounding boxes are employed in video annotation to denote the positions and identities of objects.
 105 We further track the location of solutions used throughout the experiments to track the status and

106 progress of experiments. This information is annotated by providing additional labels over container
107 object annotations (*e.g.*, ["tube_1", "LB_solution"]) for test tube with LB_solution). While exporting
108 annotations, we use a list of labels to represent the relations between the reagent and objects (*e.g.*,
109 ["tube_1", "LB_solution"]).

110 **Hierarchical structure** As for the second part, we focus on the ambiguity in the rest 9.64h videos.
111 There will be a high similarity between current practical experiments. In order to differentiate
112 these ambiguous actions, we have decided to further refine them at the granularity of human-
113 object interaction pairs in the `prc_exp`. We have divided our 🧪ProBio dataset into a three-level
114 hierarchical structure, as shown in Fig. 3. At the top level, we use brief experiment (`bf_exp`)
115 to define the overall goal of an experiment, which is only documented in the paper and works
116 in theory, *e.g.*, "yeast transformation" and "PCR preparation". Next, we use practical experiment
117 (`prc_exp`) to represent practical experiments in protocols which are composed of several Human-
118 Object Interactions (HOIs), *e.g.*, "measure OD" and "add YPD_medium into vector". Finally, we
119 use HOI pairs to define atomic operations (`act`) in experiments. In total, we obtain 13 `bf_exp`,
120 3,724 `prc_exp`, and 37,537 `act` categories. We use a triplet for HOI annotation (*e.g.*, ["human_1",
121 ["tube_2", "hold"]]) to represent the human subject id, interacting object, and the action verb. While
122 exporting annotations, we translate this annotation to a list of indexes to collect the relations between
123 humans and objects (*e.g.*, ["human_1", "object_2", "inject"]). Finally, We instruct experimenters to
124 conduct an additional round of verification to ensure the accuracy of labels, and the relationship of
125 `prc_exp` and `hoi` are shown in Fig. 4.

126 B Experiment

127 B.1 Transparent solution tracking (TansST)

128 Typically, the solution observed in BioLab exhibits characteristics of being both transparent and
129 colorless. Since the liquid can be transferred between different containers such as beakers, petri
130 dishes, and test tubes, the geometric shape of the liquid changes according to the shape of the
131 container it is housed. Hence, the monitoring of the solution is an arduous and potentially unattainable
132 undertaking. The successful execution of experiments in biology laboratories is largely dependent on
133 the transfer and fusion of solutions, making the tracking of solution a crucial and fundamental task in
134 the development of a monitoring system. In our 🧪ProBio dataset, we obtained pairs of containers
135 and solutions based on the experiment’s protocol and annotated them, facilitating the tracking of
136 the solutions. During the process of using various baselines for solution tracking, we have also
137 discovered that narrowing down the category of liquid solution types to only categories mentioned
138 in the protocols is more effective than learning-based designs (*e.g.*, fusing protocol features with
139 tracking features).

140 B.1.1 Implementation details

141 In this section, we provide details on model implementation, hyperparameters selection, and environ-
142 ment setup. We present the details for each selected model as follows:

143 Vision-only

- 144 • **TransATOM** Following the TransATOM (Fan et al., 2021a) benchmark, we first train the transpar-
145 ent solution segmentation network (Xie et al., 2020) with the TransST subset of our 🧪ProBio
146 and the easy subset of Trans10K (Fan et al., 2021a) dataset on 1 NVIDIA 3090 GPU for 40 epochs.
147 We set the initial learning rate to 0.02, batchsize as 8, and extract visual features using ResNet18.
148 In order to remain consistent with the original text, we also choose the ATOM (Danelljan et al.,
149 2019) as the tracker.
- 150 • **YOLOv5 + StrongSORT** Based on StrongSORT (Broström, 2022; Wang et al., 2022), we change
151 different detection backbones and gain final tracking results. We first finetune the yolov5n model
152 with the TransST subset of our 🧪ProBio on 1 NVIDIA 3090 GPU for 20 epochs, we have set the

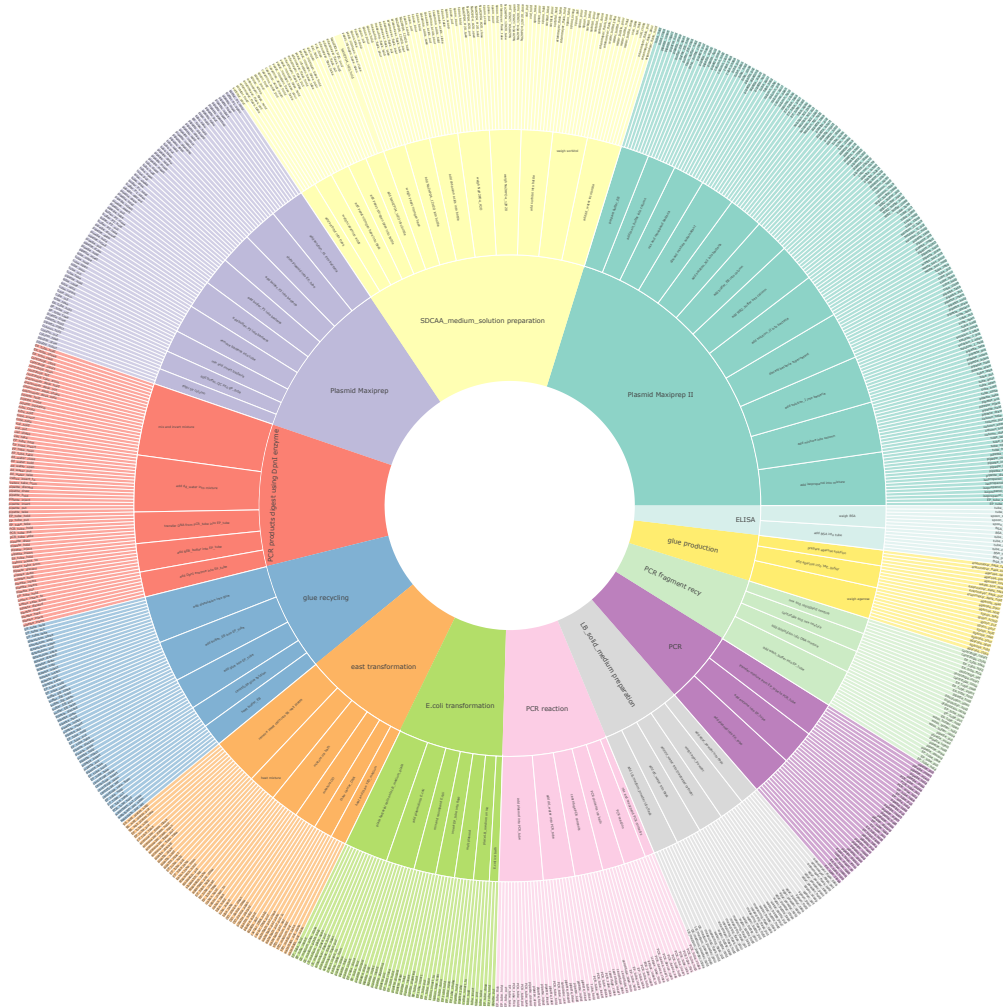


Figure 3: The three-level hierarchical structure.

153 initial learning rate to 1×10^{-5} , batchsize as 128, and the IOU threshold as 0.45. Then, we track
 154 the detected object-solution pairs with a confidence threshold of 0.25.

155 • **YOLOv7 + StrongSORT** Similar to the baseline *YOLOv5 + StrongSORT*, we first finetune yolo7-
 156 tiny model with the TransST subset of our  **ProBio** on 1 NVIDIA 3090 GPU for 20 epochs, we
 157 have set the initial learning rate to 1×10^{-5} , batchsize as 128, and the IOU threshold as 0.45. Then,
 158 we track the detected object-solution pairs with a confidence threshold of 0.25.

159 • **SAM + DeAOT** Inspired by [Chen et al. \(2023\)](#), we train a SAM-adapter based on vit_h pre-trained
 160 weights and AdamW optimizer with the TransST subset of our  **ProBio** dataset. We have set
 161 the learning rate to 2×10^{-4} , batchsize as 2. The adapter consists of two MLPs and an activate
 162 function GELU ([Hendrycks and Gimpel, 2016](#)) within two MLPs ([Liu et al., 2023](#)). We further
 163 passed the output of the adapter through a classification network, which has five *Conv2d* layers with
 164 input patch sizes of 24. We set the patch_size as 16, window_size as 14, input image resolution as
 165 1024×1024 , and train on 4 NVIDIA A100 GPUs for 20 epochs. For models with large parameter
 166 sizes like this, training adapters has shown good performance on our  **ProBio** dataset. Then, we
 167 track the detected object-solution pairs with DeAOT ([Yang and Yang, 2022](#)), choosing the model
 168 R50-DeAOT-L.

169 **Protocol-guided**

170 • **YOLOv7 + StrongSORT** Similar to the vision-only method, we first select object-solution pairs
 171 that have occurred based on the protocol of this experiment, including `prf_exp` and `prc_exp`,

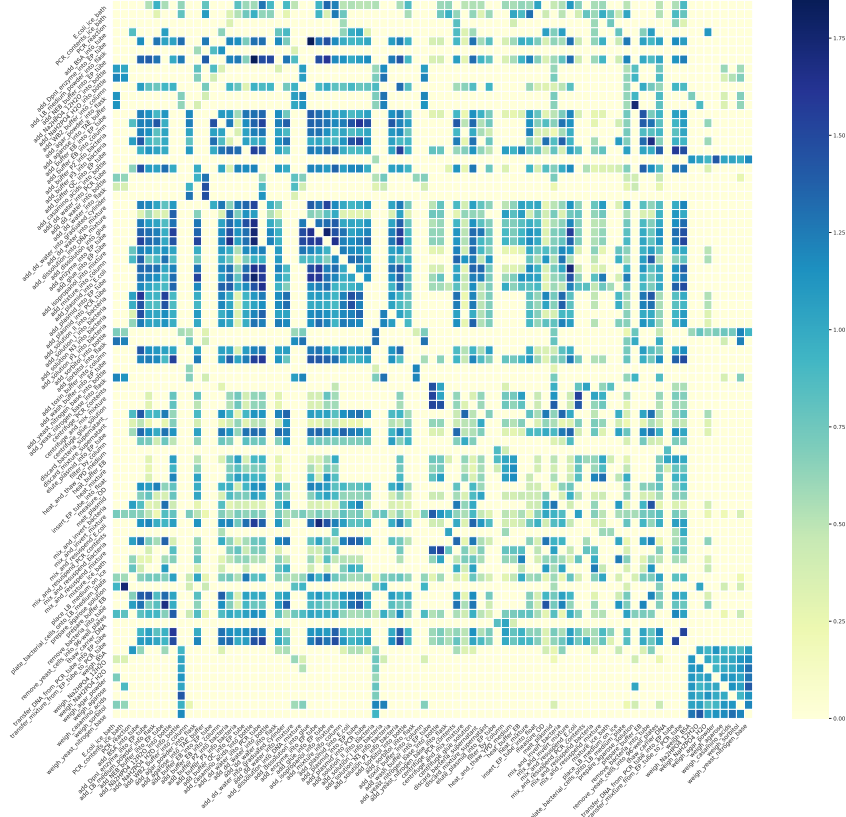


Figure 5: Visualization of the ambiguity between any two actions.

174 the IOU threshold as 0.45. Then, we track the detected object-solution pairs with the confidence
 175 threshold of 0.25.

- 176 • **SAM + DeAOT** Using the same approach as protocol-guided baseline *YOLOv7 + StrongSORT*,
 177 we first filter the desired object-solution pairs through a protocol and compile them into a list.
 178 Afterward, we perform model finetuning and subsequent tracking as baseline *SAM + DeAOT*.

179 B.2 Multimodal action recognition (MultiAR)

180 As evidenced in Section A.2.2, motions that are perceptually similar may possess distinct semantic
 181 interpretations, and practical experiments conducted across varying protocols may pertain to dissimilar
 182 meanings. In order to demonstrate the protocol-level ambiguity between two protocols in an intuitive
 183 manner, we perform a calculation of the overlap of all downstream HOI annotations. Based on the
 184 computed ambiguity metric, the complete dataset has been categorized into three distinct levels of
 185 complexity: easy, medium, and hard. Given that each level encompasses distinct practical experiments
 186 `prc_exp`, we conducted separate experiments at each level and subsequently derived conclusions.
 187 Subsequently, each of them will be explicated individually.

188 B.2.1 Ambiguity

189 With the increased granularity of action refinement, the inherent ambiguity of actions becomes
 190 apparent. However, current datasets have neglected the ambiguity present within fine-grained actions
 191 (Murray et al., 2012; Shao et al., 2020; Goyal et al., 2017; Kay et al., 2017; Zhu et al., 2022; Panda
 192 et al., 2017; Kanehira et al., 2018). Furthermore, there is currently no widely accepted metric for
 193 measuring ambiguity in actions. We find that the simplicity of using the similarity of human-object
 194 interactions `hoi` (e.g. Jaccard coefficient) to describe both the object ambiguity and procedure
 195 ambiguity is inadequate. Therefore, we define ambiguity between two actions with the bidirectional
 196 Levenshtein distance ratio, as shown in Equation (1). In Equation (1), $P(A)$ and $P(B)$ represent

197 the power set of the given A or B set of `hoi`, while `ratio` denotes the Levenshtein distance ratio.
 198 The ambiguity (*i.e.* `amb`) between two practical experiments can exceed 1, which represents a high
 199 similarity between the two `prc_exp` (shown in Fig. 5). Afterward, in order to measure the average
 200 ambiguity of each action, we define it by taking the average value (*i.e.* $\frac{1}{N} \sum_{amb \in N} amb_i$).

$$amb = \frac{1}{P(A)} * \sum_{x \in P(A)} \max_{y \in P(B)} (ratio(x, y)) + \frac{1}{P(B)} * \sum_{y \in P(B)} \max_{x \in P(A)} (ratio(y, x)) \quad (1)$$

201 B.2.2 Model Structure

202 To enhance the proficiency of the model, it is imperative to
 203 employ the technique of variable manipulation to isolate the
 204 specific components that necessitate refinement. Initially, a com-
 205 parison is made between the conversion of human-object inter-
 206 actions into descriptive text and pure vision. It is concluded that
 207 the visual modality presents a greater potential for enhancement.
 208 Subsequently, the model is enhanced through the incorporation
 209 of an alignment module and an object-centric mask module,
 210 resulting in a notable enhancement of the multimodal model’s
 211 performance. Ultimately, we substitute the concise instructions
 212 with hands-on experiments that furnish extensive insights for
 213 more intricate guidance. Fig. 6 depicts the particular operations,
 214 whereby spatial information about objects is incorporated via
 215 graph neural network (GNN) (Scarselli et al., 2008), and practical experimental information is incor-
 216 porated via SentenceBERT (Reimers and Gurevych, 2019). The calculation of similarity is performed
 217 consistently, and subsequently, the ultimate prediction outcome is generated.

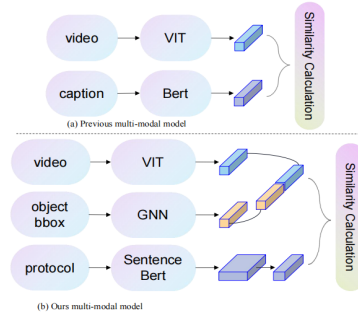


Figure 6: Structure of our action recognition module

218 B.2.3 Implementation details

219 In this section, we provide details on model implementation, hyperparameters selection, and environ-
 220 ment setup. We present the details for each selected model as follows:

221 **human study** In order to assess the viability of the two proposed benchmarks and establish the
 222 maximum attainable experimental performance, a human study was conducted with the participation
 223 of ten master’s students hailing from UC Berkeley, Peking University, and Tsinghua University. The
 224 study was bifurcated into two parts: *with protocol* and *without protocol*. The study involved the
 225 extraction of data from video recordings at varying levels of difficulty, namely easy, medium, and
 226 hard. The amount of data extracted was equivalent to 0.05 times the total of each level, and a list of
 227 79 practical experiments was provided for the participants to choose from. The experimental data
 228 pertaining to the section labeled as *without protocol* had already been prepared. For the *with protocol*
 229 part, additional information about the brief experiment to which the video belonged was provided to
 230 the participants to provide direction. All participants in the experiment were remunerated according
 231 to the criteria mentioned in Appx. A.1.

232 **Protocol-only** First, we process the detection results of human-object interaction in the video into
 233 textual form as input for subsequent steps. We then use protocol-guided techniques to predict the
 234 actions in the target video. This method helps reduce the influence of detection errors in the video
 235 and achieve the highest performance achievable at the current stage.

- 236 • **BERT** We use the pretrained BERT model and implementation provided by Hugging Face (Devlin,
 237 2018). We use the Adam optimizer Kingma and Ba (2014) and apply cross-entropy loss. We set the
 238 initial learning rate to 0.02, dropout as 0.5, batchsize as 8, and train with our descriptive text on 1
 239 NVIDIA 3090 GPU for 20 epochs.
- 240 • **SBERT** Similar to BERT, we use the pretrained SentenceBERT model and implementation provided
 241 by Hugging Face (Chiusano, 2019). On the basis of the current descriptive text, we connect the
 242 `hoi` using prompts to create a practical experiment with a sequence of operations. For example,

243 "First, we open the tube. Second, we take the pipette, etc." The generated sentences are then used
244 as training inputs for the model. We use the Adam optimizer Kingma and Ba (2014) and apply
245 cosine similarity loss. We set the initial learning rate to 2×10^{-5} , batchsize as 8, and train with our
246 descriptive text on 1 NVIDIA 3090 GPU for 20 epochs.

247 Vision-only

- 248 • **I3D Follow** (Carreira and Zisserman, 2017), ResNet50 is selected as the backbone and the frames
249 and sampling rate are set to 8. The input video undergoes a resizing process to achieve dimensions
250 of 224×224 . The Adam optimizer Kingma and Ba (2014) is employed with a weight decay of 1
251 $\times 10^{-4}$ and a uniform batch size of 64. The present model exhibits uniform settings across three
252 distinct categories and undergoes training through the utilization of a single NVIDIA A100 GPU,
253 over the course of 100 epochs.
- 254 • **SlowFast Follow** (Feichtenhofer et al., 2019), we also choose ResNet50 as the backbone and both
255 the frames and sampling rate are set to 8. The input video undergoes a resizing process to achieve
256 dimensions of 224×224 . The Adam optimizer Kingma and Ba (2014) is employed with a weight
257 decay of 1×10^{-4} and a uniform batch size of 64. The present model exhibits uniform settings
258 across three distinct categories and undergoes training through the utilization of a single NVIDIA
259 A100 GPU, over the course of 100 epochs.
- 260 • **MViT Follow** (Fan et al., 2021b), we choose MViT as the backbone and set the frames as 16,
261 sampling rate as 4. The input video undergoes a resizing process to achieve dimensions of 224×224 .
262 The AdamW optimizer Loshchilov and Hutter (2019) is employed with a weight decay of 5×10^{-2}
263 and a uniform batch size of 16. We apply soft cross entropy as the loss function. The present
264 model exhibits uniform settings across three distinct categories and undergoes training through the
265 utilization of a single NVIDIA A100 GPU, over the course of 100 epochs.
- 266 • **MViTv2 Follow** (Li et al., 2022), we choose MViT as the backbone and set the frames as 16,
267 sampling rate as 4. The input video undergoes a resizing process to achieve dimensions of 224×224 .
268 The AdamW optimizer Loshchilov and Hutter (2019) is employed with a weight decay of 5×10^{-2}
269 and a uniform batch size of 4. We apply soft cross entropy as the loss function. The present
270 model exhibits uniform settings across three distinct categories and undergoes training through the
271 utilization of a single NVIDIA A100 GPU, over the course of 100 epochs.

272 Protocol-guided (brief)

- 273 • **Vita-CLIP Follow** (Wasim et al., 2023), we finetune the pretrained CLIP model with our
274  ProBio dataset on 4 NVIDIA A100 GPUs for 50 epochs. The Adam optimizer Kingma
275 and Ba (2014) is employed with a weight decay of 5×10^{-2} and a uniform batch size of 64. We set
276 the initial learning rate to 4×10^{-4} , and the frames and sampling rate as 8.
- 277 • **EVL Follow** (Lin et al., 2022), we finetune the pretrained CLIP model with our  ProBio dataset
278 on 4 NVIDIA A100 GPUs for 50 epochs. The Adam optimizer Kingma and Ba (2014) is employed
279 with a weight decay of 5×10^{-2} and a uniform batch size of 64. We set the initial learning rate to 4
280 $\times 10^{-4}$, the frames as 32, and the sampling rate as 8.
- 281 • **ActionCLIP Follow** (Lin et al., 2022), we finetune the pretrained ViT-B model with our  ProBio
282 dataset on 1 NVIDIA 3090 GPU for 40 epochs. The AdamW optimizer Loshchilov and Hutter
283 (2019) is employed with a weight decay of 2×10^{-1} and a uniform batch size of 4. We set the
284 initial learning rate to 5×10^{-6} , the frames as 32, and the sampling rate as 8.
- 285 • **ActionCLIP + SAM** We have the same vision branch and similarity calculation module as baseline
286 *ActionCLIP*. Furthermore, we encode the object information with the graph neural network (GNN).
287 The encoder contains two parts: temporal and spatial, each composed of MLPs with different layers,
288 and ultimately outputs object features of 256 dimensions. After that, it is concatenated with the
289 image feature and inputted into the subsequent loss calculation and backpropagation module.

290 **Protocol-guided (detailed)** The input caption of the model was modified by replacing its text
291 modality with practical experiment (`prc_exp`) connected by prompts. This modified input was then
292 passed to the encoder as a text sequence. Subsequently, the text encoder in the model was substituted
293 with SentenceBERT. The training input and associated particulars pertaining to this segment of the

294 model have been expounded upon in great detail within this passage (refer to section B.2.3). The
295 following is a list solely comprised of hyperparameters:

- 296 • **Vita-CLIP** The Adam optimizer Kingma and Ba (2014) is employed with a weight decay of 5
297 $\times 10^{-2}$ and a uniform batch size of 64. We set the initial learning rate to 4×10^{-4} , and the frames
298 and sampling rate as 8.
- 299 • **EVL** The Adam optimizer Kingma and Ba (2014) is employed with a weight decay of 5×10^{-2}
300 and a uniform batch size of 64. We set the initial learning rate to 4×10^{-4} , the frames as 32, and the
301 sampling rate as 8.
- 302 • **ActionCLIP** The AdamW optimizer Loshchilov and Hutter (2019) is employed with a weight
303 decay of 2×10^{-1} and a uniform batch size of 4. We set the initial learning rate to 5×10^{-6} , the
304 frames as 32, and the sampling rate as 8.
- 305 • **ActionCLIP + SAM** The AdamW optimizer Loshchilov and Hutter (2019) is employed with a
306 weight decay of 2×10^{-1} and a uniform batch size of 4. We set the initial learning rate to 5×10^{-6} ,
307 the frames as 32, and the sampling rate as 8.

308 C Ethical review

309 **Did you describe any potential participant risks, with links to Institutional Review Board**
310 **(IRB) approvals, if applicable?** Yes, we did. We captured the daily experimental operations of
311 the researchers through ten cameras fixed on the ceiling, filming in a 24-hour uninterrupted silent
312 mode. We obtained consent from all personnel involved in the experiment and applied blur to the
313 recorded faces to ensure the confidentiality of personal information. During the data recording period,
314 no specific actions were required from the participants, and we submitted a complete set of materials
315 to the Institutional Review Board (IRB), including the list of subjects, experimental details, duration,
316 and all relevant materials.

317 C.1 Responsibility & data license

318 We bear all responsibility in case of violation of rights and our dataset is under the license of CC
319 BY-NC-SA (Attribution-NonCommercial-ShareAlike).

320 D Future work

321 First, regarding the two benchmarks proposed in this article, we have only demonstrated the effective-
322 ness of detailed protocol-guided for complex video understanding through simple experiments. There
323 is limited exploration of the model structure and the model’s performance still has a long way to go
324 to reach the oracle level. Therefore, our future work will focus on designing new models to improve
325 the performance of multimodal models in solution tracking and action recognition, further addressing
326 video understanding issues in professional scenarios. We plan to pay more attention to the alignment
327 between modalities based on improving the detection capability of the vision branch.

328 Moreover, it is more important for us to consider how to make the current dataset more widely
329 applicable. Next, we will construct a monitoring system based on the current multimodal dataset
330 to reduce the occurrence of experimental errors by experimenters, improve the repeatability and
331 correctness of experiments, curtailing expenses, and augmenting efficacy.

332 E More visualization

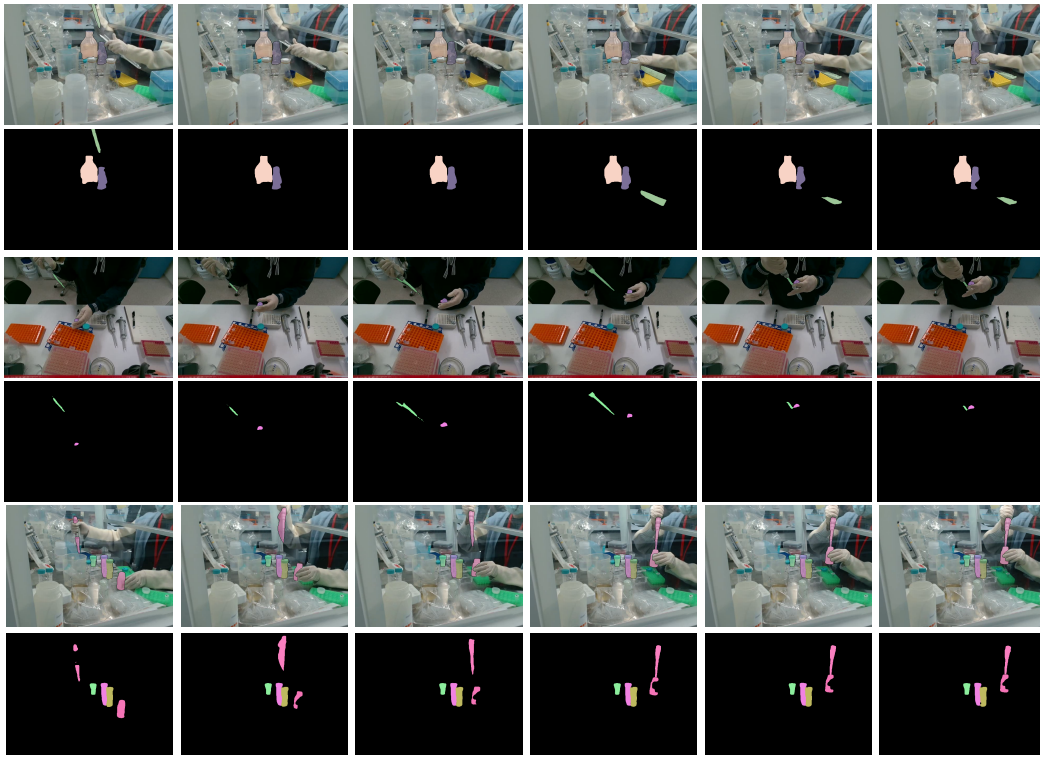


Figure 7: Visualization of the TransST results.

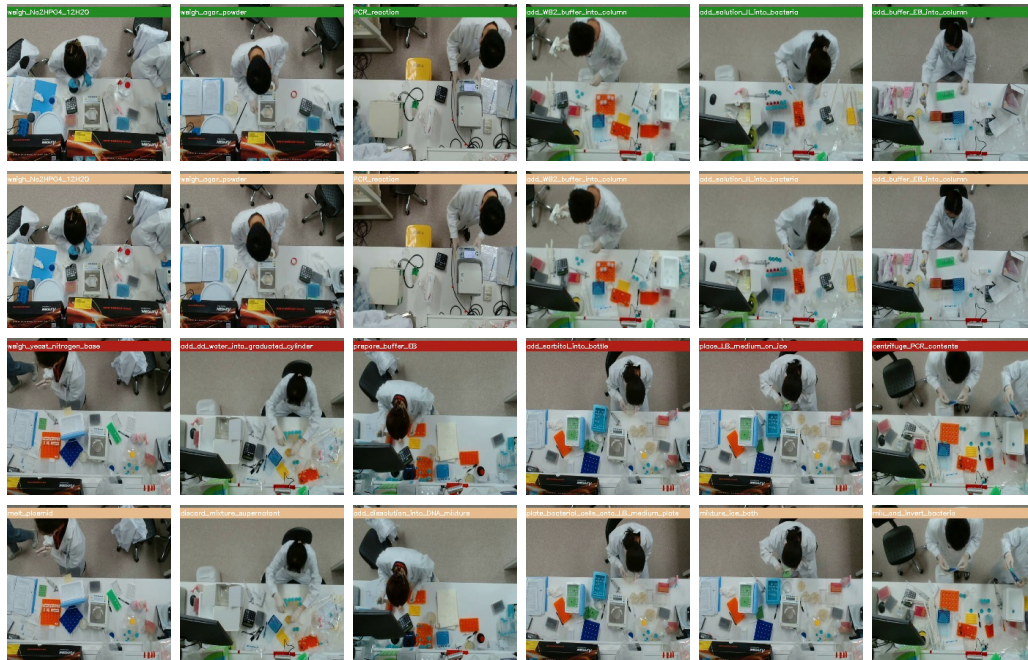


Figure 8: Visualization of the MultiAR results.

333 F Data Documentation

334 We follow the datasheet proposed in [Gebru et al. \(2021\)](#) for documenting our  ProBio and
335 associated benchmarks:

336 1. Motivation

337 (a) For what purpose was the dataset created?

338 This dataset was created to facilitate the standardization of protocols and the develop-
339 ment of intelligent monitoring systems for reducing the reproducibility crisis.

340 (b) Who created the dataset and on behalf of which entity?

341 This dataset was created by Jieming Cui, Ziren Gong, Baoxiong Jia, Siyuan Huang,
342 Zilong Zheng, Jianzhu Ma, and Yixin Zhu. Jieming Cui was a Ph.D. student at the
343 Institute for Artificial Intelligence, Peking University (PKU), Ziren Gong was a master
344 student at the School of Transportation Science and Engineering, Beihang University
345 (BUAA), Baoxiong Jia and Zilong Zheng were research scientists at National Key
346 Laboratory of General Artificial Intelligence, BIGAI (BIGAI), Jianzhu Ma was an
347 associate Professor at Department of Electronic Engineering and Institute for AI
348 Industry Research, Tsinghua University, and Yixin Zhu was an assistant professor at
349 PKU.

350 (c) Who funded the creation of the dataset?

351 The creation of this dataset was funded by PKU.

352 (d) Any other Comments?

353 None.

354 2. Composition

355 (a) What do the instances that comprise the dataset represent?

356 For video data, each instance is a video clip regularized from the raw video. These
357 raw videos are recorded from Molecular Biology Lab, and this is the first time to
358 build a multimodal video dataset in a professional biology scenario. For protocol, each
359 instance has a three-level hierarchical structure: brief experiment (`brf_exp`), practical
360 experiment (`prc_exp`), and human-object interactions (`hoi`).

361 (b) How many instances are there in total?

362 We have 3,724 videos, 13 `brf_exp`, 3,724 `prc_exp`, and 37,537 `hoi` in total.

363 (c) Does the dataset contain all possible instances or is it a sample (not necessarily random)
364 of instances from a larger set?

365 No, this is a brand-new dataset.

366 (d) What data does each instance consist of?

367 See [Appx. A.2](#).

368 (e) Is there a label or target associated with each instance?

369 See [Appx. A.2](#).

370 (f) Is any information missing from individual instances?

371 No.

372 (g) Are relationships between individual instances made explicit?

373 Video clips are related to the tasks performed in each video as well as the performers.
374 Protocols are related to the experiments in each video.

375 (h) Are there recommended data splits?

376 Yes, we have separated the whole dataset into three ambiguity levels. See [Appx. B.2](#)
377 for details.

378 (i) Are there any errors, sources of noise, or redundancies in the dataset?

379 There are almost certainly some errors in video annotations. We did our best to minimize
380 these, but some certainly remain.

381 (j) Is the dataset self-contained, or does it link to or otherwise rely on external resources
382 (e.g., websites, tweets, other datasets)?

383 The dataset is self-contained.

- 384 (k) Does the dataset contain data that might be considered confidential (e.g., data that is
385 protected by legal privilege or by doctor-patient confidentiality, data that includes the
386 content of individuals' non-public communications)?
387 No.
- 388 (l) Does the dataset contain data that, if viewed directly, might be offensive, insulting,
389 threatening, or might otherwise cause anxiety?
390 No.
- 391 (m) Does the dataset relate to people?
392 Yes, all videos are recordings of human activities and all protocols are related to these
393 activities.
- 394 (n) Does the dataset identify any subpopulations (e.g., by age, gender)?
395 No.
- 396 (o) Is it possible to identify individuals (i.e., one or more natural persons), either directly
397 or indirectly (i.e., in combination with other data) from the dataset?
398 Yes, we can recognize the actors in the original biological experiment recordings.
- 399 (p) Does the dataset contain data that might be considered sensitive in any way (e.g.,
400 data that reveals racial or ethnic origins, sexual orientations, religious beliefs, political
401 opinions or union memberships, or locations; financial or health data; biometric or
402 genetic data; forms of government identification, such as social security numbers;
403 criminal history)?
404 No.
- 405 (q) Any other comments?
406 None.

407 3. Collection Process

- 408 (a) How was the data associated with each instance acquired?
409 A team of master's and doctoral students from prestigious academic institutions such as
410 Peking University, Tsinghua University, and Peking Union Medical College Hospital
411 were recruited to conduct alignment annotation. See [Appx. A.2](#) for details.
- 412 (b) What mechanisms or procedures were used to collect the data (e.g., hardware apparatus
413 or sensor, manual human curation, software program, software API)?
414 We record videos with ten high-definition cameras and hire two teams for annotation.
415 See [Appx. A.2](#) and [Appx. A.1](#) for details.
- 416 (c) If the dataset is a sample from a larger set, what was the sampling strategy (e.g.,
417 deterministic, probabilistic with specific sampling probabilities)?
418 See [Appx. B.2](#).
- 419 (d) Who was involved in the data collection process (e.g., students, crowdworkers, contrac-
420 tors) and how were they compensated (e.g., how much were crowdworkers paid)?
421 For protocol annotations, workers are paid at a rate of 100 RMB per 30 minutes. See
422 [Appx. A.1](#) for details.
- 423 (e) Over what timeframe was the data collected?
424 The data collection process has been ongoing since 2022 and is still being updated.
- 425 (f) Were any ethical review processes conducted (e.g., by an institutional review board)?
426 Yes, see [Appx. C](#).
- 427 (g) Does the dataset relate to people?
428 Yes.
- 429 (h) Did you collect the data from the individuals in question directly, or obtain it via third
430 parties or other sources (e.g., websites)?
431 Yes, we build websites ourselves to annotate the videos and protocols.
- 432 (i) Were the individuals in question notified about the data collection?
433 Yes.
- 434 (j) Did the individuals in question consent to the collection and use of their data?
435 Yes, they were paid for these data annotations.

- 436 (k) If consent was obtained, were the consenting individuals provided with a mechanism
 437 to revoke their consent in the future or for certain uses?
 438 Yes, see [Appx. C](#).
- 439 (l) Has an analysis of the potential impact of the dataset and its use on data subjects (e.g.,
 440 a data protection impact analysis) been conducted?
 441 Yes, see [Appx. C](#).
- 442 (m) Any other comments?
 443 None.
- 444 4. Preprocessing, Cleaning and Labeling
- 445 (a) Was any preprocessing/cleaning/labeling of the data done (e.g., discretization or bucket-
 446 ing, tokenization, part-of-speech tagging, SIFT feature extraction, removal of instances,
 447 processing of missing values)?
 448 Yes, see [Appx. A.2](#).
- 449 (b) Was the "raw" data saved in addition to the preprocessed/cleaned/labeled data (e.g., to
 450 support unanticipated future uses)?
 451 Yes, we provide the raw data on our website.
- 452 (c) Is the software used to preprocess/clean/label the instances available?
 453 Yes, we provide the annotation tools on our website.
- 454 (d) Any other comments?
 455 None.
- 456 5. Uses
- 457 (a) Has the dataset been used for any tasks already?
 458 No, the dataset is newly proposed by us.
- 459 (b) Is there a repository that links to any or all papers or systems that use the dataset?
 460 Yes, we provide the link to all related information on our website.
- 461 (c) What (other) tasks could the dataset be used for?
 462 This multimodal dataset could also be used for video retrieval, text grounding, world
 463 model learning and evaluating models' compositional reasoning capabilities.
- 464 (d) Is there anything about the composition of the dataset or the way it was collected and
 465 preprocessed/cleaned/labeled that might impact future uses?
 466 We propose to annotate the before/after status of each object given a video. We believe
 467 this could serve as a general protocol for annotating changing world states.
- 468 (e) Are there tasks for which the dataset should not be used?
 469 The usage of this dataset should be limited to the scope of activity or task understanding
 470 with its various downstream tasks (e.g. anticipation, state/relationship recognition and
 471 question answering).
- 472 (f) Any other comments?
 473 None.
- 474 6. Distribution
- 475 (a) Will the dataset be distributed to third parties outside of the entity (e.g., company,
 476 institution, organization) on behalf of which the dataset was created?
 477 Yes, the dataset will be made publicly available.
- 478 (b) How will the dataset will be distributed (e.g., tarball on website, API, GitHub)?
 479 The dataset could be accessed on our website.
- 480 (c) When will the dataset be distributed?
 481 The dataset will be released to the public upon acceptance of this paper. We provide
 482 private links for the review process.
- 483 (d) Will the dataset be distributed under a copyright or other intellectual property (IP)
 484 license, and/or under applicable terms of use (ToU)?
 485 We release our benchmark under CC BY-NC-SA² license.

²<https://paperswithcode.com/datasets/license>

- 486 (e) Have any third parties imposed IP-based or other restrictions on the data associated
487 with the instances?
488 No.
- 489 (f) Do any export controls or other regulatory restrictions apply to the dataset or to
490 individual instances?
491 No.
- 492 (g) Any other comments?
493 None.
- 494 7. Maintenance
- 495 (a) Who is supporting/hosting/maintaining the dataset?
496 Jieming Cui is maintaining.
- 497 (b) How can the owner/curator/manager of the dataset be contacted (e.g., email address)?
498 jeremy.cuij@gmail.com
- 499 (c) Is there an erratum?
500 Currently, no. As errors are encountered, future versions of the dataset may be released
501 and updated on our website.
- 502 (d) Will the dataset be updated (e.g., to correct labeling errors, add new instances, delete
503 instances)?
504 Yes.
- 505 (e) If the dataset relates to people, are there applicable limits on the retention of the data
506 associated with the instances (e.g., were individuals in question told that their data
507 would be retained for a fixed period of time and then deleted)?
508 No.
- 509 (f) Will older versions of the dataset continue to be supported/hosted/maintained?
510 Yes, older versions of the benchmark will be maintained on our website.
- 511 (g) If others want to extend/augment/build on/contribute to the dataset, is there a mechanism
512 for them to do so?
513 Yes, errors may be submitted to us through email.
- 514 (h) Any other comments?
515 None.

516 References

- 517 Begley, C. G. and Ellis, L. M. (2012). Raise standards for preclinical cancer research. *Nature*. 1
- 518 Broström, M. (2022). Real-time multi-camera multi-object tracker using yolov5 and strongsort with osnet.
519 https://github.com/mikel-brostrom/Yolov5_StrongSORT_OSNet. 5
- 520 Cao, Z., Simon, T., Wei, S.-E., and Sheikh, Y. (2017). Realtime multi-person 2d pose estimation using part
521 affinity fields. In *Conference on Computer Vision and Pattern Recognition (CVPR)*. 3
- 522 Carreira, J. and Zisserman, A. (2017). Quo vadis, action recognition? a new model and the kinetics dataset. In
523 *Conference on Computer Vision and Pattern Recognition (CVPR)*. 10
- 524 Chen, T., Zhu, L., Ding, C., Cao, R., Zhang, S., Wang, Y., Li, Z., Sun, L., Mao, P., and Zang, Y. (2023). Sam
525 fails to segment anything?—sam-adapter: Adapting sam in underperformed scenes: Camouflage, shadow, and
526 more. *arXiv preprint arXiv:2304.09148*. 6
- 527 Chiusano, F. (2019). [https://huggingface.co/sentence-transformers/
528 all-MiniLM-L6-v2](https://huggingface.co/sentence-transformers/all-MiniLM-L6-v2). 9
- 529 Danelljan, M., Bhat, G., Khan, F. S., and Felsberg, M. (2019). Atom: Accurate tracking by overlap maximization.
530 In *Conference on Computer Vision and Pattern Recognition (CVPR)*. 5
- 531 Devlin, J. (2018). <https://huggingface.co/bert-base-uncased>. 9
- 532 Fan, H., Miththanathaya, H. A., Rajan, S. R., Liu, X., Zou, Z., Lin, Y., Ling, H., et al. (2021a). Transparent object
533 tracking benchmark. In *International Conference on Computer Vision (ICCV)*. 5
- 534 Fan, H., Xiong, B., Mangalam, K., Li, Y., Yan, Z., Malik, J., and Feichtenhofer, C. (2021b). Multiscale vision
535 transformers. *arXiv preprint arXiv:2104.11227*. 10
- 536 Feichtenhofer, C., Fan, H., Malik, J., and He, K. (2019). Slowfast networks for video recognition. In *International
537 Conference on Computer Vision (ICCV)*. 10
- 538 Gebru, T., Morgenstern, J., Vecchione, B., Vaughan, J. W., Wallach, H., Iii, H. D., and Crawford, K. (2021).
539 Datasheets for datasets. *Communications of the ACM*. 13
- 540 Goyal, R., Ebrahimi Kahou, S., Michalski, V., Materzynska, J., Westphal, S., Kim, H., Haenel, V., Freund, I.,
541 Yianilos, P., Mueller-Freitag, M., et al. (2017). The "something something" video database for learning and
542 evaluating visual common sense. In *International Conference on Computer Vision (ICCV)*. 8
- 543 Hendrycks, D. and Gimpel, K. (2016). Gaussian error linear units (gelus). *arXiv preprint arXiv:1606.08415*. 6
- 544 Ioannidis, J. P. (2005). Why most published research findings are false. *PLoS Medicine*. 1
- 545 JOVE (2006). <https://www.jove.com/>. 1
- 546 Kanehira, A., Van Gool, L., Ushiku, Y., and Harada, T. (2018). Aware video summarization. In *Conference on
547 Computer Vision and Pattern Recognition (CVPR)*. 8
- 548 Kay, W., Carreira, J., Simonyan, K., Zhang, B., Hillier, C., Vijayanarasimhan, S., Viola, F., Green, T., Back, T.,
549 Natsev, P., et al. (2017). The kinetics human action video dataset. *arXiv preprint arXiv:1705.06950*. 8
- 550 Kingma, D. P. and Ba, J. (2014). Adam: A method for stochastic optimization. *arXiv preprint arXiv:1412.6980*.
551 9, 10, 11
- 552 Li, Y., Wu, C.-Y., Fan, H., Mangalam, K., Xiong, B., Malik, J., and Feichtenhofer, C. (2022). Mvitv2: Improved
553 multiscale vision transformers for classification and detection. In *International Conference on Computer
554 Vision (ICCV)*. 10
- 555 Lin, Z., Geng, S., Zhang, R., Gao, P., de Melo, G., Wang, X., Dai, J., Qiao, Y., and Li, H. (2022). Frozen clip
556 models are efficient video learners. *arXiv preprint arXiv:2208.03550*. 10
- 557 Liu, W., Shen, X., Pun, C.-M., and Cun, X. (2023). Explicit visual prompting for low-level structure segmenta-
558 tions. In *Conference on Computer Vision and Pattern Recognition (CVPR)*. 6
- 559 Loshchilov, I. and Hutter, F. (2019). Decoupled weight decay regularization. In *Proceedings of the 33rd
560 Conference on Neural Information Processing Systems*, pages 8024–8035. 10, 11
- 561 MDPI (2011). <https://www.mdpi.com/journal/cells>. 1

- 562 Murray, N., Marchesotti, L., and Perronnin, F. (2012). Ava: A large-scale database for aesthetic visual analysis.
563 In *Conference on Computer Vision and Pattern Recognition (CVPR)*. 8
- 564 NATURE (2000). <https://protocolexchange.researchsquare.com/>. 1
- 565 Nest.Bio Labs (2023). <https://www.nest.bio/>. 3
- 566 Panda, R., Das, A., Wu, Z., Ernst, J., and Roy-Chowdhury, A. K. (2017). Weakly supervised summarization of
567 web videos. In *International Conference on Computer Vision (ICCV)*. 8
- 568 Reimers, N. and Gurevych, I. (2019). Sentence-bert: Sentence embeddings using siamese bert-networks. *arXiv*
569 *preprint arXiv:1908.10084*. 9
- 570 Scarselli, F., Gori, M., Tsoi, A. C., Hagenbuchner, M., and Monfardini, G. (2008). The graph neural network
571 model. *IEEE transactions on neural networks*. 9
- 572 Shao, D., Zhao, Y., Dai, B., and Lin, D. (2020). Finegym: A hierarchical video dataset for fine-grained action
573 understanding. In *Conference on Computer Vision and Pattern Recognition (CVPR)*. 8
- 574 Ultralytics (2022). ultralytics/yolov5: v7.0 - YOLOv5 SOTA Realtime Instance Segmentation. [https:](https://github.com/ultralytics/yolov5.com)
575 [//github.com/ultralytics/yolov5.com](https://github.com/ultralytics/yolov5.com). Accessed: 7th May, 2023. 3
- 576 Wang, C.-Y., Bochkovskiy, A., and Liao, H.-Y. M. (2022). YOLOv7: Trainable bag-of-freebies sets new
577 state-of-the-art for real-time object detectors. *arXiv preprint arXiv:2207.02696*. 5
- 578 Wasim, S. T., Naseer, M., Khan, S., Khan, F. S., and Shah, M. (2023). Vita-clip: Video and text adaptive clip via
579 multimodal prompting. In *Conference on Computer Vision and Pattern Recognition (CVPR)*. 10
- 580 Xie, E., Wang, W., Wang, W., Ding, M., Shen, C., and Luo, P. (2020). Segmenting transparent objects in the
581 wild. In *European Conference on Computer Vision (ECCV)*. 5
- 582 Yang, Z. and Yang, Y. (2022). Decoupling features in hierarchical propagation for video object segmentation. In
583 *Advances in Neural Information Processing Systems (NeurIPS)*. 6
- 584 Zhu, W., Lu, J., Han, Y., and Zhou, J. (2022). Learning multiscale hierarchical attention for video summarization.
585 *Pattern Recognition*, 122:108312. 8